Interface laws for multi-physic composites

Michèle Serpilli, Raffaella Rizzoni, Serge Dumont, Frédéric Lebon

Interface Laws for Multi-physic Composites

Michele Serpilli[1(✉)], Raffaella Rizzoni[2], Serge Dumont[3], and Frédéric Lebon[4]

[1] Department of Civil and Building Engineering, and Architecture, Università Politecnica delle Marche, Via brecce bianche, 60131 Ancona, Italy
m.serpilli@univpm.it
[2] Department of Engineering, University of Ferrara, Via Saragat 1, 44122 Ferrara, Italy
raffaella.rizzoni@unife.it
[3] University of Nîmes, IMAG, CNRS UMR 5149 Pl. E. Bataillon, 34095 Montpellier Cedex 5, France
serge.dumont@unimes.fr
[4] Aix-Marseille University, CNRS, Centrale Marseille, LMA, Impasse Nikola Tesla 4, Marseille, France
lebon@lma.cnrs-mrs.fr

Abstract. The paper describes the mechanical behavior of a composite constituted by two solids, bonded by a thin adhesive layer in a general multi-physic framework, by employing the asymptotic expansion technique. After defining a small parameter ε, which will tend to zero, associated with the thickness and the constitutive coefficients of the intermediate layer, we characterize three different limit models and their associated limit problems: the soft interface model, in which the constitutive coefficients depend linearly on ε; the hard interface model, in which the constitutive properties are independent of ε; the rigid interface model, in which they depend on $\frac{1}{\varepsilon}$. The asymptotic expansion method is reviewed by taking into account the effect of higher order terms and by defining a general multi-physic interface law which comprises the above aforementioned models. Moreover, the FEM implementation of the transmission model is presented through a numerical example.

Keywords: Composites · Interfaces · Multi-physic materials · Asymptotic analysis

1 Introduction

In the last decades, the interest in bonded structures, obtained by assembling different parts made of possibly different materials to compose a unique structure, is strongly increased. The advantage of such composites is that their mechanical performances and properties are designed to be superior to those of the constituent materials acting independently. In the present work we focus our attention to a specific type of composite, constituted by two media, called the

adherents, bonded together with a thin interphase layer, called the adhesive. We assume that the composite constituents are made of different multi-physic materials with highly contrasted constitutive properties. The study considers a generic multi-physic coupling in a very general framework and can be adapted to well-known multi-physic behaviors, such as piezoelectricity, thermo-elasticity, as well as to multifield microstructural theories, such as micropolar elasticity. The analysis has been carried out by means of the asymptotic expansions method. This technique has been applied to the rigorous derivation of simplified models for complex assemblies, presenting thin interphases, in the field of linear elasticity [1–3] as well as in piezoelectricity, taking into account other physical interactions [4–6]. The asymptotic methods allow to replace the adhesive layer with a two-dimensional surface, the so-called imperfect interface, with non-classical transmission conditions between the two adherents. By defining a small parameter ε, associated with the thickness and constitutive properties of the middle layer, we perform an asymptotic analysis. We assume that the middle layer thickness depends linearly on ε, while the multi-physic stiffness ratios between the adherents and the adhesive depend on ε^p. We identify three critical exponents p, corresponding to different imperfect interface models: $p = 1$, the soft (also called lowly-conducting) multi-physic interface model; $p = 0$, the hard (also called moderately-conducting) multi-physic interface model; $p = -1$, the rigid (also called highly-conducting) multi-physic interface model. Following the approach by [3], we characterize the order zero and higher order transmission problems. Finally, a general multi-physic interface model is developed, and numerically tested through the finite element method. In particular, in the framework of piezoelectricity, we compare the results obtained by modeling the adhesive as an interphase, having a thin finite thickness, with the results obtained with the general multi-physic interface model.

2 Statement of the Problem

Let us define a small dimensionless parameter $0 < \varepsilon < 1$. We consider the assembly constituted of two solids $\Omega_{\pm}^{\varepsilon} \subset \mathbb{R}^3$, called the adherents, bonded together by an intermediate thin layer $B^{\varepsilon} := S \times (-\frac{\varepsilon}{2}, \frac{\varepsilon}{2})$ of thickness ε, called the adhesive, with cross-section $S \subset \mathbb{R}^2$. In the following B^{ε} and S will be called interphase and interface, respectively. Let $S_{\pm}^{\varepsilon}$ be the plane contact surfaces between the adhesive and the adherents and let $\Omega^{\varepsilon} := \Omega_{+}^{\varepsilon} \cup B^{\varepsilon} \cup \Omega_{-}^{\varepsilon}$ denote the composite system comprising the interphase and the adherents (cf. Fig. 1a).

We suppose that the composite is constituted by a multi-physic material, in which different physical behaviors interact together, such as in piezoelectricity. Its equilibrium state is determined by a collection of order parameters $\mathbf{s}^{\varepsilon} := (\mathbf{u}_1^{\varepsilon}, \ldots, \mathbf{u}_N^{\varepsilon}, \varphi_1^{\varepsilon}, \ldots, \varphi_M^{\varepsilon})$: N vector state variables, namely $\mathbf{u}_i^{\varepsilon}$, and M scalar state variables, namely φ_k^{ε}. With the multi-physic state $\mathbf{s}^{\varepsilon}$, we associate its conjugated physical quantity $\mathbf{t}^{\varepsilon} = \mathbf{t}^{\varepsilon}(\boldsymbol{\nabla}^{\varepsilon}\mathbf{s}^{\varepsilon})$, where $\boldsymbol{\nabla}^{\varepsilon}\mathbf{s}^{\varepsilon}$ denotes the gradient of $\mathbf{s}^{\varepsilon}$. The vector field $\mathbf{t}^{\varepsilon} := (\boldsymbol{\sigma}_1^{\varepsilon}, \ldots, \boldsymbol{\sigma}_N^{\varepsilon}, \mathbf{D}_1^{\varepsilon}, \ldots, \mathbf{D}_M^{\varepsilon})$ represents a generalized stress field. We also consider the following homogeneous and linear constitutive law:

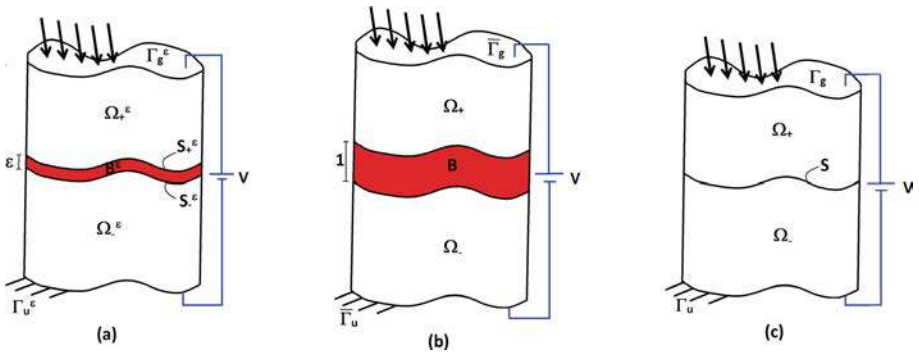

Fig. 1. Initial (a), rescaled (b) and limit (c) configurations of the composite.

$$\mathbf{t}^\varepsilon = \mathbb{K}^\varepsilon \boldsymbol{\nabla}^\varepsilon \mathbf{s}^\varepsilon,$$

where $\mathbb{K}^\varepsilon$ is a generalized linear constitutive matrix. The constitutive tensor $\mathbb{K}^\varepsilon$ satisfies suitable symmetry and positivity properties.

We assume that the adherents are subject to a generalized system of body forces $\mathbf{F}^\varepsilon : \Omega^\varepsilon_\pm \to \mathbb{R}^{3N\times M}$ and surface forces $\mathbf{G}^\varepsilon : \Gamma^\varepsilon_g \to \mathbb{R}^{3N\times M}$, where $\Gamma^\varepsilon_g \subset (\partial\Omega^\varepsilon_+ \setminus S^\varepsilon_+)\cup(\partial\Omega^\varepsilon_- \setminus S^\varepsilon_-)$. Body and surface forces are neglected in adhesive layer. On $\Gamma^\varepsilon_u := (\partial\Omega^\varepsilon_+ \setminus S^\varepsilon_+)\cup(\partial\Omega^\varepsilon_- \setminus S^\varepsilon_-)\setminus\Gamma^\varepsilon_g$ homogeneous boundary conditions are prescribed, so that $\mathbf{s}^\varepsilon = \mathbf{0}$ on Γ^ε_u. We assume that on $\Gamma_{lat} := \partial S \times (-\frac{\varepsilon}{2}, \frac{\varepsilon}{2})$ homogeneous Neumann boundary conditions are applied. The differential formulation of the governing equations has the following structure:

$$\begin{cases} -\text{div } \mathbf{t}^\varepsilon = \mathbf{F}^\varepsilon \text{ in } \Omega^\varepsilon, \\ \mathbf{t}^\varepsilon \mathbf{n}^\varepsilon = \mathbf{G}^\varepsilon \quad \text{on } \Gamma^\varepsilon_g, \\ \mathbf{s}^\varepsilon = \mathbf{0} \quad\quad \text{on } \Gamma^\varepsilon_u, \end{cases} \tag{1}$$

where $\mathbf{t}^\varepsilon\mathbf{n}^\varepsilon := (\boldsymbol{\sigma}^\varepsilon_1\mathbf{n}^\varepsilon, \dots, \boldsymbol{\sigma}^\varepsilon_N\mathbf{n}^\varepsilon, \mathbf{D}^\varepsilon_1\cdot\mathbf{n}^\varepsilon, \dots, \mathbf{D}^\varepsilon_M\cdot\mathbf{n}^\varepsilon)$ represents the generalized traction vector on the boundary Γ^ε_g and $\mathbf{n}^\varepsilon$ the outer normal unit vector to Γ^ε_g. Let us introduce the functional space $V(\Omega^\varepsilon) := \{\mathbf{s}^\varepsilon \in H^1(\Omega^\varepsilon;\mathbb{R}^{3N\times M});\ \mathbf{s}^\varepsilon = \mathbf{0} \text{ on } \Gamma^\varepsilon_u\}$. The variational formulation of problem (1) defined on the variable domain Ω^ε can be written as follows:

$$\begin{cases} \text{Find } \mathbf{s}^\varepsilon \in V(\Omega^\varepsilon) \text{ such that} \\ \bar{A}^\varepsilon_-(\mathbf{s}^\varepsilon,\mathbf{r}^\varepsilon) + \bar{A}^\varepsilon_+(\mathbf{s}^\varepsilon,\mathbf{r}^\varepsilon) + \hat{A}^\varepsilon(\mathbf{s}^\varepsilon,\mathbf{r}^\varepsilon) = L^\varepsilon(\mathbf{r}^\varepsilon), \end{cases} \tag{2}$$

for all $\mathbf{r}^\varepsilon := (\mathbf{v}^\varepsilon_1, \dots, \mathbf{v}^\varepsilon_N, \psi^\varepsilon_1, \dots, \psi^\varepsilon_M) \in V(\Omega^\varepsilon)$, where defined by

$$\bar{A}^\varepsilon_\pm(\mathbf{s}^\varepsilon,\mathbf{r}^\varepsilon) := \int_{\Omega^\varepsilon_\pm} \bar{\mathbb{K}}^\varepsilon \boldsymbol{\nabla}^\varepsilon \mathbf{s}^\varepsilon \cdot \boldsymbol{\nabla}^\varepsilon \mathbf{r}^\varepsilon dx^\varepsilon, \quad \hat{A}^\varepsilon(\mathbf{s}^\varepsilon,\mathbf{r}^\varepsilon) := \int_{B^\varepsilon} \hat{\mathbb{K}}^\varepsilon \boldsymbol{\nabla}^\varepsilon \mathbf{s}^\varepsilon \cdot \boldsymbol{\nabla}^\varepsilon \mathbf{r}^\varepsilon dx^\varepsilon,$$
$$L^\varepsilon(\mathbf{r}^\varepsilon) := \int_{\Omega^\varepsilon_\pm} \mathbf{F}^\varepsilon \cdot \mathbf{r}^\varepsilon dx^\varepsilon + \int_{\Gamma^\varepsilon_g} \mathbf{G}^\varepsilon \cdot \mathbf{r}^\varepsilon d\Gamma^\varepsilon.$$

3 The Asymptotic Expansions Method

In order to perform an asymptotic analysis of problem (2) when ε tends to zero, we rewrite the problem on a fixed domain Ω independent of ε. By using the approach of [7], we consider the change of variables $\pi^\varepsilon : x \in \overline{\Omega} \mapsto x^\varepsilon \in \overline{\Omega}^\varepsilon$ given by

$$\pi^\varepsilon : \begin{cases} \bar{\pi}^\varepsilon(x_1, x_2, x_3) = (x_1, x_2, x_3 \mp \frac{1}{2}(1-\varepsilon)), \text{ for all } x \in \overline{\Omega}_\pm, \\ \hat{\pi}^\varepsilon(x_1, x_2, x_3) = (x_1, x_2, \varepsilon x_3), \qquad\qquad \text{for all } x \in \overline{B}, \end{cases}$$

where, after the change of variables, the adherents occupy $\Omega_\pm := \Omega^\varepsilon_\pm \pm \frac{1}{2}(1-\varepsilon)\mathbf{e}_3$ and the interphase $B = \{x \in \mathbb{R}^3 : \ (x_1, x_2) \in S, \ |x_3| < \frac{1}{2}\}$. The sets $S_\pm = \{x \in \mathbb{R}^3 : \ (x_1, x_2) \in S, \ x_3 = \pm\frac{1}{2}\}$ denote the interfaces between B and $\Omega_\pm$ and $\Omega = \Omega_+ \cup \Omega_- \cup B$ is the rescaled configuration of the composite. Lastly, Γ_g and Γ_u indicate the images through π^ε of Γ^ε_g and Γ^ε_u (cf. Fig. 1b). Consequently, $\frac{\partial}{\partial x^\varepsilon_\alpha} = \frac{\partial}{\partial x_\alpha}$ and $\frac{\partial}{\partial x^\varepsilon_3} = \frac{\partial}{\partial x_3}$ in $\Omega_\pm$, $\frac{\partial}{\partial x^\varepsilon_\alpha} = \frac{\partial}{\partial x_\alpha}$ and $\frac{\partial}{\partial x^\varepsilon_3} = \frac{1}{\varepsilon}\frac{\partial}{\partial x_3}$ in B.

We assume that the constitutive coefficients of $\Omega^\varepsilon_\pm$ are independent of ε, $\bar{\mathbb{K}}^\varepsilon = \bar{\mathbb{K}}$, while the constitutive coefficients of B^ε depend on ε, $\hat{\mathbb{K}}^\varepsilon = \varepsilon^p \hat{\mathbb{K}}$, with $p \in \{-1, 0, 1\}$. Three different limit behaviors will be characterized according to the choice of the exponent p: in the case of $p = -1$, we derive a model for a *rigid* interface; when $p = 0$, we derive a model for a *hard* interface; by choosing $p = 1$, we deduce a model for a *soft* interface. Finally, we suppose that the forces are such that $L^\varepsilon(\mathbf{r}^\varepsilon) = L(\mathbf{r})$. By virtue of the previous hypothesis, the rescaled problem can be written in the following form:

$$\begin{cases} \text{Find } \mathbf{s}^\varepsilon \in V(\Omega), \text{ such that} \\ \bar{A}_-(\mathbf{s}^\varepsilon, \mathbf{r}) + \bar{A}_+(\mathbf{s}^\varepsilon, \mathbf{r}) + \varepsilon^{p-1}\hat{a}(\mathbf{s}^\varepsilon, \mathbf{r}) + \varepsilon^p \hat{b}(\mathbf{s}^\varepsilon, \mathbf{r}) + \varepsilon^{p+1}\hat{c}(\mathbf{s}^\varepsilon, \mathbf{r}) = L(\mathbf{r}), \end{cases} \tag{3}$$

for all $\mathbf{r} \in V(\Omega) := \{\mathbf{s} \in H^1(\Omega; \mathbb{R}^{3N\times M}); \ \mathbf{s} = \mathbf{0} \ \text{ on } \Gamma_u\}$, where

$$\bar{A}_\pm(\mathbf{s}^\varepsilon, \mathbf{r}) := \int_{\Omega_\pm} \bar{\mathbb{K}}\boldsymbol{\nabla}\mathbf{s}^\varepsilon \cdot \boldsymbol{\nabla}\mathbf{r} dx, \qquad \hat{a}(\mathbf{s}^\varepsilon, \mathbf{r}) := \int_B \hat{\mathbb{K}}_{33}\mathbf{s}^\varepsilon_{,3} \cdot \mathbf{r}_{,3} dx,$$
$$\hat{b}(\mathbf{s}^\varepsilon, \mathbf{r}) := \int_B \left\{\hat{\mathbb{K}}_{3\alpha}\mathbf{s}^\varepsilon_{,3} \cdot \mathbf{r}_{,\alpha} + \hat{\mathbb{K}}_{\alpha 3}\mathbf{s}^\varepsilon_{,\alpha} \cdot \mathbf{r}_{,3}\right\} dx, \quad \hat{c}(\mathbf{s}^\varepsilon, \mathbf{r}) := \int_B \hat{\mathbb{K}}_{\alpha\beta}\mathbf{s}^\varepsilon_{,\beta} \cdot \mathbf{r}_{,\alpha} dx,$$

and $\hat{\mathbb{K}}_{ij}$ denote the sub-matrices of $\hat{\mathbb{K}}$, defined by

$$\hat{\mathbb{K}} = \begin{bmatrix} \hat{\mathbb{K}}_{\alpha\beta} & \hat{\mathbb{K}}_{\alpha 3} \\ \hat{\mathbb{K}}_{3\alpha} & \hat{\mathbb{K}}_{33} \end{bmatrix}, \quad (\hat{\mathbb{K}}_{ij})^T = \hat{\mathbb{K}}_{ji}.$$

We can now perform an asymptotic analysis of the rescaled problem (3). Since the rescaled problem (3) has a polynomial structure with respect to the small parameter ε, we can look for the solution $\mathbf{s}^\varepsilon$ of the problem as a series of powers of ε:

$$\mathbf{s}^\varepsilon = \mathbf{s}^0 + \varepsilon\mathbf{s}^1 + \varepsilon^2\mathbf{s}^2 + \ldots, \ \ \bar{\mathbf{s}}^\varepsilon = \bar{\mathbf{s}}^0 + \varepsilon\bar{\mathbf{s}}^1 + \varepsilon^2\bar{\mathbf{s}}^2 + \ldots, \ \ \hat{\mathbf{s}}^\varepsilon = \hat{\mathbf{s}}^0 + \varepsilon\hat{\mathbf{s}}^1 + \varepsilon^2\hat{\mathbf{s}}^2 + \ldots. \tag{4}$$

where $\bar{\mathbf{s}}^\varepsilon = \mathbf{s}^\varepsilon \circ \bar{\pi}^\varepsilon$ and $\hat{\mathbf{s}}^\varepsilon = \mathbf{s}^\varepsilon \circ \hat{\pi}^\varepsilon$. By substituting (4) into the rescaled problem (3), and by identifying the terms with identical power of ε, we obtain, as customary, a set of variational problems to be solved in order to characterize the limit multi-physic state $\mathbf{s}^0$, the first order corrector term $\mathbf{s}^1$ and their associated limit problem, for $p \in \{-1, 0, 1\}$.

Following the approach described in [2,3], we introduce the matching conditions based on the continuity of the generalized traction $\mathbf{t}^\varepsilon \mathbf{e}_3$ and multiphysic state $\mathbf{s}^\varepsilon$ at the interfaces $S^\varepsilon_\pm$ in the initial configuration and on the continuity of the traction and state $\bar{\mathbf{t}}^\varepsilon \mathbf{e}_3$, $\bar{\mathbf{s}}^\varepsilon$, $\hat{\mathbf{t}}^\varepsilon \mathbf{e}_3$, $\hat{\mathbf{s}}^\varepsilon$ at the interfaces $S_\pm$ in the rescaled configuration. Hence, one has

$$\begin{array}{ll} [[\mathbf{s}^\varepsilon]] = [\bar{\mathbf{s}}^\varepsilon] - \varepsilon \langle\langle \mathbf{s}^\varepsilon_{,3} \rangle\rangle + o(\varepsilon), & \langle\langle \mathbf{s}^\varepsilon \rangle\rangle = \langle \bar{\mathbf{s}}^\varepsilon \rangle - \frac{\varepsilon}{4} [[\mathbf{s}^\varepsilon_{,3}]], \\ [[\mathbf{t}^\varepsilon \mathbf{e}_3]] = [\bar{\mathbf{t}}^\varepsilon \mathbf{e}_3] - \varepsilon \langle\langle \mathbf{t}^\varepsilon_{,3} \mathbf{e}_3 \rangle\rangle + o(\varepsilon), & \langle\langle \mathbf{t}^\varepsilon \mathbf{e}_3 \rangle\rangle = \langle \bar{\mathbf{t}}^\varepsilon \mathbf{e}_3 \rangle - \frac{\varepsilon}{4} [[\mathbf{t}^\varepsilon_{,3} \mathbf{e}_3]], \end{array} \tag{5}$$

where

$$\begin{array}{l} \langle f \rangle(\tilde{x}) := \frac{1}{2}(f(\tilde{x}, (1/2)^+) + f(\tilde{x}, -(1/2)^-), \quad \tilde{x} := (x_\alpha) \in S, \\ [f]\,(\tilde{x}) := f(\tilde{x}, (1/2)^+) - f(\tilde{x}, -(1/2)^-), \\ \langle\langle f \rangle\rangle(\tilde{x}) := \frac{1}{2}(f(\tilde{x}, 0^+) + f(\tilde{x}, 0^-)), \\ [[f]](\tilde{x}) := f(\tilde{x}, 0^+) - f(\tilde{x}, 0^-), \end{array}$$

denote, respectively, the mean value and the jump functions at the interfaces.

4 The Multi-physic Interface Models

In this section we present the asymptotic models for multi-physic interfaces obtained for the soft, hard and rigid cases at order 0 and order 1. For the sake of brevity, we will skip all the mathematical technicalities and computations connected with the derivation of the limit models.

4.1 The Soft Multi-physic Interface

The transmission problems at order 0 and order 1 can be summarized as follows:

- Order 0

Governing equations

$$\begin{cases} -\text{div}\ \bar{\mathbf{t}}^0 = \mathbf{F} & \text{in } \Omega_\pm, \\ \bar{\mathbf{t}}^0 \mathbf{n} = \mathbf{G} & \text{on } \Gamma_g, \\ \bar{\mathbf{s}}^0 = \mathbf{0} & \text{on } \Gamma_u, \end{cases}$$

Transmission conditions on $S_\pm$

$$\begin{cases} [\bar{\mathbf{s}}^0] = (\hat{\mathbb{K}}_{33})^{-1} \langle \bar{\mathbf{t}}^0 \mathbf{e}_3 \rangle, \\ [\bar{\mathbf{t}}^0 \mathbf{e}_3] = \mathbf{0}. \end{cases}$$

- Order 1

Governing equations

$$\begin{cases} -\text{div}\ \bar{\mathbf{t}}^1 = \mathbf{0} & \text{in } \Omega_\pm, \\ \bar{\mathbf{t}}^1 \mathbf{n} = \mathbf{0} & \text{on } \Gamma_g, \\ \bar{\mathbf{s}}^1 = \mathbf{0} & \text{on } \Gamma_u, \end{cases}$$

Transmission conditions on $S_\pm$

$$\begin{cases} [\bar{\mathbf{s}}^1] = (\hat{\mathbb{K}}_{33})^{-1} \left(\langle \bar{\mathbf{t}}^1 \mathbf{e}_3 \rangle - \hat{\mathbb{K}}_{\alpha 3} \langle \bar{\mathbf{s}}^0 \rangle_{,\alpha} \right), \\ [\bar{\mathbf{t}}^1 \mathbf{e}_3] = -\hat{\mathbb{K}}_{3\alpha} [\bar{\mathbf{s}}^0]_{,\alpha}. \end{cases}$$

The transmission problems for a soft multi-physic interface at order 0 and order 1 represent a formal generalization of the soft interface models obtained by means of the asymptotic methods in linear elasticity [2,3] and in other multi-field frameworks, such as piezoelectricity [4], magneto-electro-thermo-elasticity [5] and micropolar elasticity [6]. The soft interface model presents the same structure at both order 0 and 1 as, for instance, in linear elastic asymptotic models. At order 0, the interface shows a discontinuity of the multi-physic state and behaves from a mechanical point of view as a series of linear springs, reacting to the gap between the top and bottom multi-physic states, while the generalized traction vector remains continuous. At order 1, we obtain a mixed interface model in which both the multi-physic state and the traction vector are discontinuous through the interface and they depend on the in-plane derivatives of the jump and mean values of $\bar{\mathbf{s}}^0$.

4.2 The Hard Multi-physic Interface

The hard interface transmission problems at order 0 and order 1 take the following expressions:

- Order 0

Governing equations

$$\begin{cases} -\text{div } \bar{\mathbf{t}}^0 = \mathbf{F} & \text{in } \Omega_\pm, \\ \bar{\mathbf{t}}^0 \mathbf{n} = \mathbf{G} & \text{on } \Gamma_g, \\ \bar{\mathbf{s}}^0 = \mathbf{0} & \text{on } \Gamma_u, \end{cases}$$

Transmission conditions on $S_\pm$

$$\begin{cases} [\bar{\mathbf{s}}^0] = \mathbf{0}, \\ [\bar{\mathbf{t}}^0 \mathbf{e}_3] = \mathbf{0}. \end{cases}$$

- Order 1

Governing equations

$$\begin{cases} -\text{div } \bar{\mathbf{t}}^1 = \mathbf{0} & \text{in } \Omega_\pm, \\ \bar{\mathbf{t}}^1 \mathbf{n} = \mathbf{0} & \text{on } \Gamma_g, \\ \bar{\mathbf{s}}^1 = \mathbf{0} & \text{on } \Gamma_u, \end{cases}$$

Transmission conditions on $S_\pm$

$$\begin{cases} [\bar{\mathbf{s}}^1] = (\hat{\mathbb{K}}_{33})^{-1} \left(\langle \bar{\mathbf{t}}^0 \mathbf{e}_3 \rangle - \hat{\mathbb{K}}_{\alpha 3} \langle \bar{\mathbf{s}}^0 \rangle_{,\alpha} \right), \\ [\bar{\mathbf{t}}^1 \mathbf{e}_3] = - \left(\hat{\mathbb{K}}_{3\alpha} [\bar{\mathbf{s}}^1]_{,\alpha} + \hat{\mathbb{K}}_{\alpha\beta} \langle \bar{\mathbf{s}}^0 \rangle_{,\alpha\beta} \right). \end{cases}$$

It is interesting to notice that the hard multi-physic interface problems is equivalent to the ones derived in the case of linear elasticity [1–3]. Indeed, according to the order 0 model, the interface conditions reduce to classical continuity conditions of the multi-physic state and of its associated generalized traction vector. In this case, the model does not capture the presence of the intermediate layer and the adherents are perfectly bonded together: this particular behavior is typical of adhesives having the same rigidity properties of the top and bottom bodies. At order 1, we encounter a mixed interface model with a jump of the state and traction vector depending on the values of the multi-physic state and traction vector at order 0. These order 0 terms, being known from the solution of the previous problem, can be viewed as external source terms.

4.3 The Rigid Multi-physic Interface

The differential formulations of the rigid interface problems at order 0 and order 1 take the following form:

- Order 0

Governing equations

$$\begin{cases} -\text{div } \bar{\mathbf{t}}^0 = \mathbf{F} & \text{in } \Omega_\pm, \\ \bar{\mathbf{t}}^0 \mathbf{n} = \mathbf{G} & \text{on } \Gamma_g, \\ \bar{\mathbf{s}}^0 = \mathbf{0} & \text{on } \Gamma_u, \end{cases}$$

Transmission conditions on $S_\pm$

$$\begin{cases} [\bar{\mathbf{s}}^0] = \mathbf{0}, \\ [\bar{\mathbf{t}}^0 \mathbf{e}_3] = -\hat{\mathbb{L}}_{\alpha\beta} \langle \bar{\mathbf{s}}^0 \rangle_{,\alpha\beta}. \end{cases}$$

- Order 1

Governing equations

$$\begin{cases} -\text{div } \bar{\mathbf{t}}^1 = \mathbf{0} & \text{in } \Omega_\pm, \\ \bar{\mathbf{t}}^1 \mathbf{n} = \mathbf{0} & \text{on } \Gamma_g, \\ \bar{\mathbf{s}}^1 = \mathbf{0} & \text{on } \Gamma_u, \end{cases}$$

Transmission conditions on $S_\pm$

$$\begin{cases} [\bar{\mathbf{s}}^1] = -(\hat{\mathbb{K}}_{33})^{-1} \hat{\mathbb{K}}_{\alpha 3} \langle \bar{\mathbf{s}}^0 \rangle_{,\alpha}, \\ [\bar{\mathbf{t}}^1 \mathbf{e}_3] = -\hat{\mathbb{K}}_{3\alpha} (\hat{\mathbb{K}}_{33})^{-1} \langle \bar{\mathbf{t}}^0 \mathbf{e}_3 \rangle_{,\alpha} - \hat{\mathbb{L}}_{\alpha\beta} \langle \bar{\mathbf{s}}^1 \rangle_{,\alpha\beta}, \end{cases}$$

where $\hat{\mathbb{L}}_{\alpha\beta} := \hat{\mathbb{K}}_{\alpha\beta} - \hat{\mathbb{K}}_{3\alpha} (\hat{\mathbb{K}}_{33})^{-1} \hat{\mathbb{K}}_{\beta 3}$. The rigid multi-physic interface problems show the same features of the rigid interface asymptotic models obtained in different frameworks in [4–6, 8]. Concerning the order 0 model, we obtain a continuity of the multi-physic state at the interface level, while the traction vector is discontinuous and depends on the divergence of a generalized membrane stress vector $\mathbf{N}^0_\alpha := \hat{\mathbb{L}}_{\alpha\beta} \langle \bar{\mathbf{s}}^0 \rangle_{,\beta}$. The order 1 presents a discontinuity on both the multi-physic state and traction vector. Analogously to the order 0 model, we obtain a generalized equilibrium membrane problem defined on the plane of the interface.

4.4 The General Multi-physic Interface

The approach of [3] can be extended in order to obtain a condensed form of the transmission conditions summarizing both the orders 0 and 1 of the soft, hard and rigid cases in only one couple of equations in terms of the jump of the multi-physic state and generalized tractions at the interface.

Therefore, we denote by $\tilde{\mathbf{s}}^\varepsilon := \bar{\mathbf{s}}^0 + \varepsilon \bar{\mathbf{s}}^1 + \varepsilon^2 \bar{\mathbf{s}}^2$ and $\tilde{\mathbf{t}}^\varepsilon := \bar{\mathbf{t}}^0 + \varepsilon \bar{\mathbf{t}}^1$, two suitable approximations for $\bar{\mathbf{s}}^\varepsilon$ and $\bar{\mathbf{t}}^\varepsilon$. Let us consider the rigid multiphysics interface conditions, as starting point. After rescaling back the constitutive coefficients $\hat{\mathbb{K}} = \varepsilon \hat{\mathbb{K}}^\varepsilon$ in B^ε, we can write $[\tilde{\mathbf{s}}^\varepsilon]$ and $[\tilde{\mathbf{t}}^\varepsilon \mathbf{e}_3]$. Indeed, one has

$$\begin{aligned} [\tilde{\mathbf{s}}^\varepsilon] &:= [\bar{\mathbf{s}}^0] + \varepsilon [\bar{\mathbf{s}}^1] + \varepsilon^2 [\bar{\mathbf{s}}^2] = -\varepsilon (\hat{\mathbb{K}}^\varepsilon_{33})^{-1} \left(\hat{\mathbb{K}}^\varepsilon_{\alpha 3} \langle \tilde{\mathbf{s}}^\varepsilon \rangle_{,\alpha} - \langle \tilde{\mathbf{t}}^\varepsilon \mathbf{e}_3 \rangle \right) + o(\varepsilon^2), \\ \left[\tilde{\mathbf{t}}^\varepsilon \mathbf{e}_3 \right] &:= [\bar{\mathbf{t}}^0 \mathbf{e}_3] + \varepsilon [\bar{\mathbf{t}}^1 \mathbf{e}_3] = -\varepsilon \hat{\mathbb{K}}^\varepsilon_{3\alpha} (\hat{\mathbb{K}}^\varepsilon_{33})^{-1} \langle \tilde{\mathbf{t}}^\varepsilon \mathbf{e}_3 \rangle_{,\alpha} - \varepsilon \hat{\mathbb{L}}^\varepsilon_{\alpha\beta} \langle \tilde{\mathbf{s}}^\varepsilon \rangle_{,\alpha\beta} + o(\varepsilon^2). \end{aligned}$$

An alternative expression of the above transmission conditions can be given in terms of $\langle \tilde{\mathbf{t}}^\varepsilon \mathbf{e}_3 \rangle$ and $\left[\tilde{\mathbf{t}}^\varepsilon \mathbf{e}_3 \right]$, which will be useful to write the variational formulation of the interface multiphysics problem:

$$\begin{aligned} \langle \tilde{\mathbf{t}}^\varepsilon \mathbf{e}_3 \rangle &= \tfrac{1}{\varepsilon} \hat{\mathbb{K}}^\varepsilon_{33} [\tilde{\mathbf{s}}^\varepsilon] + \hat{\mathbb{K}}^\varepsilon_{\alpha 3} \langle \tilde{\mathbf{s}}^\varepsilon \rangle_{,\alpha} + o(\varepsilon^2), \\ \left[\tilde{\mathbf{t}}^\varepsilon \mathbf{e}_3 \right] &= -\hat{\mathbb{K}}^\varepsilon_{3\alpha} [\tilde{\mathbf{s}}^\varepsilon]_{,\alpha} - \varepsilon \hat{\mathbb{K}}^\varepsilon_{\alpha\beta} \langle \tilde{\mathbf{s}}^\varepsilon \rangle_{,\alpha\beta} + o(\varepsilon^2). \end{aligned} \tag{6}$$

It is easy to prove that this interface law is general enough to describe the interface laws at order 0 and order 1 prescribing the multi-physic state jump and traction jump in the cases of the soft and hard interfaces, by choosing the following scalings for the constitutive matrices: $\hat{\mathbb{K}}^\varepsilon = \varepsilon\hat{\mathbb{K}}$, for the soft case, and $\hat{\mathbb{K}}^\varepsilon = \hat{\mathbb{K}}$, for the hard case.

The relations (6) can be transformed into interface equations defined on S, by making use of the matching relations (5), up to higher order terms:

$$\begin{array}{l} \langle\langle \mathbf{t}\mathbf{e}_3 \rangle\rangle = \frac{1}{\varepsilon}\hat{\mathbb{K}}_{33}[[\mathbf{s}]] + \hat{\mathbb{K}}_{\alpha 3}\langle\langle \mathbf{s}\rangle\rangle_{,\alpha}, \\ [[\mathbf{t}\mathbf{e}_3]] = -\hat{\mathbb{K}}_{3\alpha}[[\mathbf{s}]]_{,\alpha} - \varepsilon\hat{\mathbb{K}}_{\alpha\beta}\langle\langle \mathbf{s}\rangle\rangle_{,\alpha\beta}. \end{array} \tag{7}$$

5 Finite Element Implementation and Numerical Test

In order to derive the variational form of the multi-physic problem, which will be numerically tested through a finite element procedure, one can write the variational form of the equilibrium problem on each sub-domain Ω_+ and Ω_-:

$$\begin{aligned} &\int_{\Omega_\pm} \bar{\mathbb{K}}\boldsymbol{\nabla}\mathbf{s}\cdot\boldsymbol{\nabla}\mathbf{r}dx - \int_S \mathbf{t}(\tilde{x},0^+)\mathbf{n}(\tilde{x},0^+)\cdot\mathbf{r}d\Gamma - \int_S \mathbf{t}(\tilde{x},0^-)\mathbf{n}(\tilde{x},0^-)\cdot\mathbf{r}d\Gamma \\ &= \int_{\Omega_\pm}\mathbf{F}\cdot\mathbf{r}dx + \int_{\Gamma_g}\mathbf{G}\cdot\mathbf{r}d\Gamma, \end{aligned}$$

which can be rewritten as

$$\int_{\Omega_\pm} \bar{\mathbb{K}}\boldsymbol{\nabla}\mathbf{s}\cdot\boldsymbol{\nabla}\mathbf{r}dx + \int_S [[\mathbf{t}\mathbf{e}_3\cdot\mathbf{r}]]d\tilde{x} = L(\mathbf{r}),$$

letting $\mathbf{e}_3 = \mathbf{n}(\tilde{x},0^-) = -\mathbf{n}(\tilde{x},0^+)$ and $d\Gamma = d\tilde{x}$. Then, using the property $[[ab]] = \langle\langle a\rangle\rangle[[b]] + [[a]]\langle\langle b\rangle\rangle$, relations (7) and after an integration by parts, we obtain

$$\begin{cases} \text{Find } \mathbf{s}\in W(\tilde{\Omega}), \text{ such that} \\ \bar{A}_-(\mathbf{s},\mathbf{r}) + \bar{A}_+(\mathbf{s},\mathbf{r}) + \mathcal{A}(\mathbf{s},\mathbf{r}) = \mathcal{L}(\mathbf{r}), \end{cases} \tag{8}$$

for all $\mathbf{r}\in W(\tilde{\Omega}) := \{\mathbf{s}\in H^1(\tilde{\Omega};\mathbb{R}^{3N\times M}),\ \mathbf{s}|_S \in H^1(S;\mathbb{R}^{3N\times M}), \mathbf{s}=\mathbf{0} \text{ on } \Gamma_u\}$, with $\tilde{\Omega} := \Omega_+\cup S\cup\Omega_-$ and

$$\begin{aligned} \mathcal{A}(\mathbf{s},\mathbf{r}) &:= \int_S \left(\frac{1}{\varepsilon}\hat{\mathbb{K}}_{33}[[\mathbf{s}]]\cdot[[\mathbf{r}]] + \hat{\mathbb{K}}_{\alpha 3}\langle\langle\mathbf{s}\rangle\rangle_{,\alpha}\cdot[[\mathbf{r}]] + \hat{\mathbb{K}}_{3\alpha}[[\mathbf{s}]]\cdot\langle\langle\mathbf{r}\rangle\rangle_{,\alpha} + \varepsilon\hat{\mathbb{K}}_{\alpha\beta}\langle\langle\mathbf{s}\rangle\rangle_{,\alpha}\cdot\langle\langle\mathbf{r}\rangle\rangle_{,\beta}\right)d\tilde{x}, \\ \mathcal{L}(\mathbf{r}) &:= \int_{\partial\Omega_\pm}\mathbf{F}\cdot\mathbf{r}dx + \int_{\Gamma_g}\mathbf{G}\cdot\mathbf{r}d\Gamma. \end{aligned}$$

A standard finite element method is employed to solve this equation. In order to take into account the jumps in the displacements across the interface, a "flat" finite element is considered on the interface S that has all nodes on S, the first ones related to Ω_-, and the other ones related to Ω_+. It is then possible to write a stiffness matrix of this problem that is invertible and with standard error estimates (for more details, see for example [9]).

5.1 Numerical Study: The Piezoelectric Composite Plate

The aim of this study is to numerically test the general interface law, expressed in (8), comparing it to a three-dimensional analysis of the problem. As preliminary test, we consider the piezoelectric case. The piezoelectric state at the equilibrium is determined by the pair $\mathbf{s} := (\mathbf{u}, \varphi)$, where $\mathbf{u}$ and φ represent the displacement field and the electric potential. The generalized stress vector is given by $\mathbf{t} := (\boldsymbol{\sigma}, \mathbf{D})$, where $\boldsymbol{\sigma}$ and $\mathbf{D}$ denote, respectively, the Cauchy stress tensor and the electric displacement.

Let us consider a piezoelectric three-phases composite plate, which occupies a 3D domain defined by $\Omega = [0, L_1] \times [0, L_2] \times [-h/2, h/2]$, with $L_1 = 10h$ and $L_2 = 5h$ (see Fig. 2). The adhesive thickness is set to be ε.

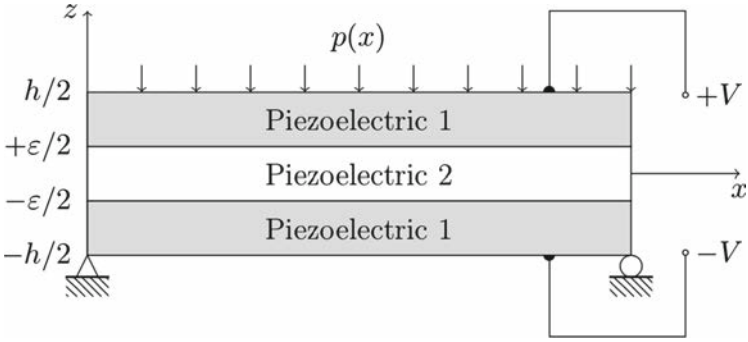

Fig. 2. The geometry of the piezoelectric composite plate in the plane (x, z).

The adherents are constituted by PVDF (Polyvinylidene fluoride), a monoclinic piezoelectric material with poling axis $\mathbf{e}_3$, while the adhesive is made of PZT-4, a transversally isotropic piezoelectric material with poling axis $\mathbf{e}_3$. This constitutive sub-matrices $(\mathbb{K}_{ij})$ are defined as follows:

$$\mathbb{K}_{33} = \begin{pmatrix} 2c_{55} & 0 & 0 & 0 \\ 0 & 2c_{44} & 0 & 0 \\ 0 & 0 & c_{33} & e_{33} \\ 0 & 0 & -e_{33} & H_{33} \end{pmatrix}, \quad \mathbb{K}_{12} = \begin{pmatrix} 0 & 2c_{66} + c_{12} & 0 & 0 \\ 0 & 0 & 0 & 0 \\ 0 & 0 & 0 & 0 \\ 0 & 0 & 0 & 0 \end{pmatrix},$$

$$\mathbb{K}_{13} = \begin{pmatrix} 0 & 0 & 2c_{55} & e_{15} \\ 0 & 0 & 0 & 0 \\ c_{13} & 0 & 0 & 0 \\ -e_{31} & 0 & 0 & 0 \end{pmatrix}, \quad \mathbb{K}_{23} = \begin{pmatrix} 0 & 0 & 0 & 0 \\ 0 & 0 & 2c_{44} & e_{24} \\ 0 & c_{23} & 0 & 0 \\ 0 & -e_{32} & 0 & 0 \end{pmatrix},$$

$$\mathbb{K}_{11} = \begin{pmatrix} c_{11} & 0 & 0 & 0 \\ 0 & 2c_{66} & 0 & 0 \\ 0 & 0 & 2c_{55} & e_{15} \\ 0 & 0 & -e_{15} & H_{11} \end{pmatrix}, \quad \mathbb{K}_{22} = \begin{pmatrix} 2c_{66} & 0 & 0 & 0 \\ 0 & c_{22} & 0 & 0 \\ 0 & 0 & 2c_{44} & e_{24} \\ 0 & 0 & -e_{24} & H_{22} \end{pmatrix}.$$

For a transversally isotropic material with poling axis $\mathbf{e}_3$, one has $c_{11} = c_{22}$, $c_{13} = c_{23}$, $c_{55} = c_{44}$, $c_{66} = (c_{11} - c_{12})/2$, $e_{15} = e_{24}$, $e_{31} = e_{32}$ and $H_{11} = H_{22}$. The elastic, dielectric and piezoelectric coefficients are listed in Table 1. The piezoelectric composite plate is subject to an electric potential difference equal to $V = 50\,\mathrm{V}$ at the top and bottom faces, as shown in Fig. 2. We assume that no mechanical body and surface loads are applied. In this case, the composite plates behaves as an actuator (see [10]).

Table 1. Piezoelectric material properties

Moduli	PZT-4	PVDF
c_{11}, GPa	139	238.24
c_{22}, GPa	139	23.6
c_{33}, GPa	115	10.64
c_{12}, GPa	77.8	3.98
c_{13}, GPa	74.3	2.19
c_{23}, GPa	74.3	1.92
$2c_{44}$, GPa	25.6	2.15
$2c_{55}$, GPa	25.6	4.4
$2c_{66}$, GPa	30.6	6.43
e_{31}, $\mathrm{C/m^2}$	−5.2	−0.13
e_{32}, $\mathrm{C/m^2}$	−5.2	−0.145
e_{33}, $\mathrm{C/m^2}$	15.1	−0.276
e_{24}, $\mathrm{C/m^2}$	12.7	−0.009
e_{15}, $\mathrm{C/m^2}$	12.7	−0.135
H_{11}, nF/m	13.06	0.111
H_{22}, nF/m	13.06	0.106
H_{33}, nF/m	11.51	0.106

The finite element simulations (made with GetFEM) are carried out using Q1 elements, with 7280 nodes (29203 degrees of freedom) for the three phases problem and 5824 nodes (23379 degrees of freedom) for the problem with the interface law.

First, the influence of the relative thickness of the interphase $\frac{\varepsilon}{L}$ is investigated in order to evaluate the accuracy of the various modeling proposed in the previous sections. In particular, the quality of the solutions is evaluated considering the L^2-relative error $e = \frac{\|\mathbf{s}^\varepsilon - \mathbf{s}_{model}\|}{\|\mathbf{s}^\varepsilon\|}$, where $\mathbf{s}^\varepsilon$ denotes the reference solution computed using the three-phases problem with a fine finite element mesh, while $\mathbf{s}_{model}$ indicates the solution of the interface model (8). The convergence of the general interface model towards the three-phases one with respect to the thickness ratio $\frac{\varepsilon}{L}$ is presented in Fig. 3. From the plot, it can be observed that, by

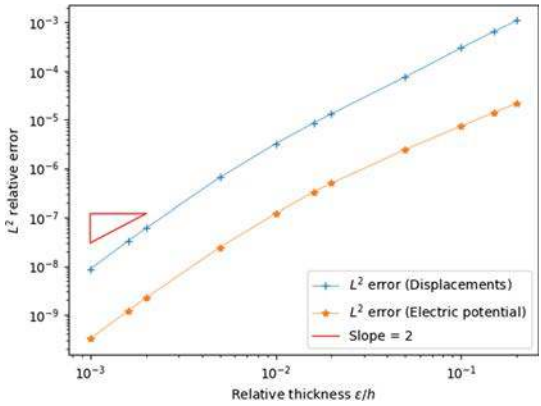

Fig. 3. Convergence results with respect to the thickness $\frac{\varepsilon}{L}$.

reducing the thickness of the adhesive, the relative error has a drastic reduction and so, the proposed general interface model provides an acceptable solution and it is able to correctly approximate the solution $\mathbf{s}^\varepsilon$. The convergence rate is ε^2. Besides, even if the relative thickness is of 1%, the relative error is equal to $7.65 \cdot 10^{-2}$% for the displacement field and $9.06 \cdot 10^{-4}$% for the electric potential, meaning that the general interface model can also be used for moderately thick adhesive layers.

Now, let us fix the relative thickness $\frac{\varepsilon}{L} = 0.1$. The numerical results for the variables are provided using the dimensionless units. For an applied electric potential V, we set:

$$(U_i, \Phi) = \frac{E_0}{V}(u_i, \frac{\varphi}{E_0}) \qquad (T_{ij}, \mathcal{D}_k) = \frac{hE_0}{C_{00}V}(\sigma_{ij}, E_0 D_k),$$

where we have chosen, for numerical convenience, $E_0 = 10^9\,\mathrm{Vm}^{-1}$ and $C_{00} = 1\,\mathrm{GPa}$. The results are represented in Figs. 4, 5 and 6.

Figure 4 represents the trend of the displacement field and electric potential, evaluated in $x = L_1/2, y = L_2/2, z/h \in [-0.5, 0.5]$. The plot shows a good agreement between the solution of the general interface problem (dotted line) and the solution of the three-phases problem (solid line). The composite plate behaves mostly as a Kirchhoff-Love single-layer plate, taking also into account the transversal deformation of the adhesive. From the electric point of view, the electric potential is linear through the adherents and constant through the adhesive: this is due to the fact that the intermediate layer (PZT-4) has a higher electrical conductivity with respect to upper and lower bodies (PVDF), see Table 1, and, hence, it behaves as a highly conducting interface.

Figures 5 and 6 represent the trend of the jumps of the displacement and electric potential and the jumps of the stress vector and normal electric displacement along the x-axis, namely $(x \in [0, L_1], y = L_2/2, z = 0)$, and y-axis, namely $(x = L_1/2, y =\in [0, L_2], z = 0)$. The numerical simulations highlight

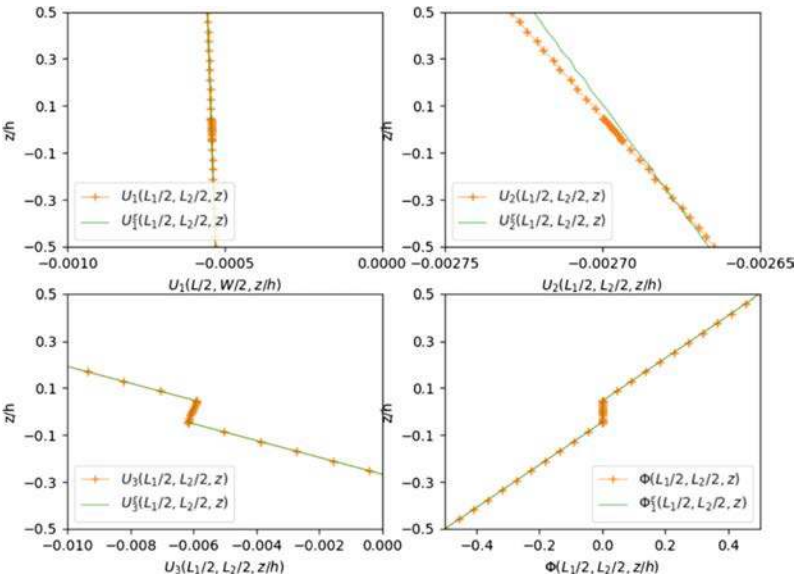

Fig. 4. Representation of the displacements and the electric potential on a section along the z-axis.

that the proposed model is able to describe the mechanical behavior of the composite. Few solution oscillations can be found close to the lateral boundaries, due to the presence of edges, which produce expected stress concentrations and singularities.

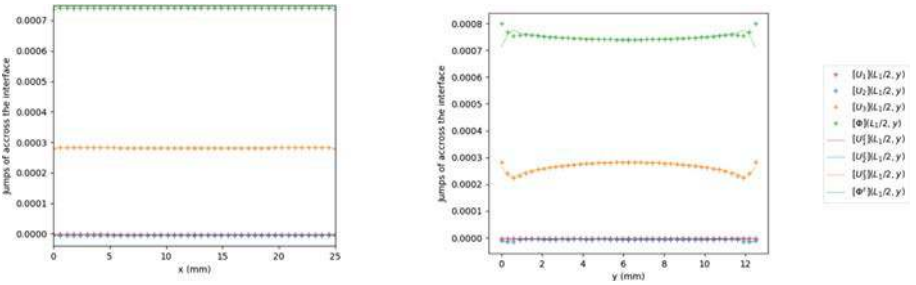

Fig. 5. Representation of the jumps in the displacements and the electric potential across the interface on a section along the x-axis and y-axis.

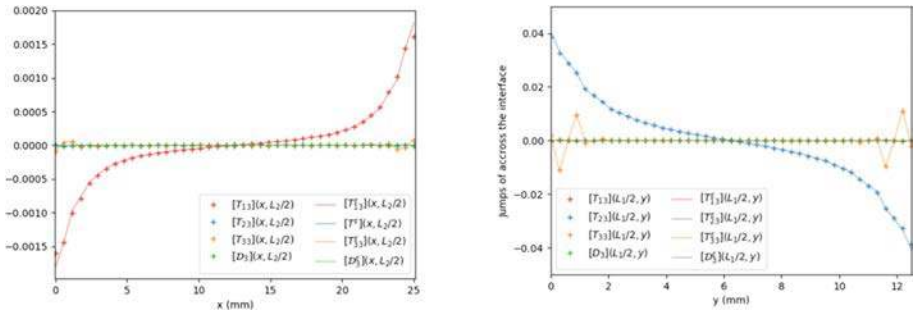

Fig. 6. Representation of the jumps of the stress vector and normal electric displacement across the interface on a section along the x-axis and y-axis.

6 Concluding Remarks

General imperfect contact conditions have been proposed, simulating the behavior of a thin interphase undergoing linear coupled multiphysics phenomena. These conditions link the generalized traction vector field and its jump to the multiphysic state vector field and its jump at the interface, which is the geometric limit of the interphase as its thickness parameter ε goes to zero. Three interface models (soft, hard and rigid) have been deduced by means of the asymptotic methods, by varying the rigidity ratios between the adhesive and adherents and considering the order 0 and order 1 corrector terms. Furthermore, these three different models have been condensed in one general imperfect interface model and its variational formulation has been presented. The weak formulation represents a key step towards the FEM simulation. A numerical example has been presented considering a piezoelectric composite plate, subject to an electric potential difference at the top and bottom faces. The numerical results show the convergence of the solution of the three-phases model towards the solution of the proposed model as ε tends to zero, highlighting the accuracy and "goodness" of the general interface conditions.

References

1. Lebon, F., Rizzoni, R.: Asymptotic analysis of a thin interface: the case involving similar rigidity. Int. J. Eng. Sci. **48**, 473–486 (2010)
2. Dumont, S., Rizzoni, R., Lebon, F., Sacco, E.: Soft and hard interface models for bonded elements. Compos. Part B Eng. **153**, 480–490 (2018)
3. Rizzoni, R., Dumont, S., Lebon, F., Sacco, E.: Higher order model for soft and hard elastic interfaces. Int. J. Solids Struct. **51**, 4137–4148 (2014)
4. Serpilli, M.: Mathematical modeling of weak and strong piezoelectric interfaces. J. Elast. **121**(2), 235–254 (2015)
5. Serpilli, M.: Asymptotic interface models in magneto-electro-thermo-elastic composites. Meccanica **52**(6), 1407–1424 (2017)

6. Serpilli, M.: On modeling interfaces in linear micropolar composites. Math. Mech. Solids **23**(4), 667–685 (2018)
7. Ciarlet, P.G.: Mathematical Elasticity, vol. II: Theory of Plates. North-Holland, Amsterdam (1997)
8. Bessoud, A.-L., Krasucki, F., Michaille, G.: Multi-materials with strong interface: variational modelings. Asymptot. Anal. **1**, 1–19 (2009)
9. Nairn, J.A.: Numerical implementation of imperfect interfaces. Comput. Mater. Sci. **40**, 525–536 (2007)
10. Bonaldi, F., Geymonat, G., Krasucki, F., Serpilli, M.: An asymptotic plate model for magneto-electro-thermo-elastic sensors and actuators. Math. Mech. Solids **22**(4), 798–822 (2017)